29 Mar 2001, 7:30 pm - 9:30 pm

Fluidization Behavior of Silty Soils in the Shear Zone Base on Ring Shear Tests

Gonghui Wang
Kyoto University, Japan

Kyoji Sassa
Kyoto University, Japan

FLUIDIZATION BEHAVIOR OF SILTY SOILS IN THE SHEAR ZONE BASED ON RING SHEAR TESTS

Gonghui Wang
Landslide Section, DPRI Kyoto University,
Uji, Kyoto, Japan 611-0011

Kyoji Sassa
Landslide Section, DPRI Kyoto University,
Uji, Kyoto, Japan 611-0011

ABSTRACT

Using a newly developed large ring-shear apparatus, a series of tests was conducted on silty soils to study their undrained shear behavior. The samples were made by mixing loess into a fine-grained silica sand with 10, 20, and 30% loess by weight. By performing tests at different initial void ratio, the undrained shear behavior of samples with different loess contents at loose and medium-dense states was presented and discussed. Basing on the tests results, effects of loess contents on the peak and residual shear strengths are examined. It was found that adding loess into the host sand could lower the peak and residual shear strengths; and these two strengths decreases with increasing loess content. Meanwhile, with increasing loess content, the dissipation of generated pore pressure from the shear zone becomes remarked slower when the shear box was turned into drained conditions, and there is little, if any, dissipation for tests on the mixture with 30% loess.

KEYWORDS

Fluidization, pore water pressure, shear-zone, grain-crushing, silty soils, ring shear test

INTRODUCTION

A fluidized landslide is usually characterized by high mobility and long run-out distance, and then followed by tremendous hazards. It is always the result of liquefaction, a process during which high pore water pressure is generated and soil mass loses a great part of its strength and shows the behavior of liquid. Therefore, research on this kind of failure has been mainly focused on liquefaction potential analysis with emphasis on the undrained shear behavior of soils. By now there are countless experimental studies, which have been conducted on clean sand, and the undrained shear behavior of clean sand has been made relatively clear. However, compared with those tests on clean sand, the undrained shear behavior of silty soils is less studied, although it has been pointed out that silt and silt-clay mixture are more prone to suffer from liquefaction failure with large resulting run-out distance, basing on many field observations (Bishop, 1973; Eckersley, 1990; Ishihara, et al., 1990; Zlatovic and Ishihara, 1995). As stated by Guo and Prakash (1999), for evaluating the liquefaction potential of this kind of soil, there is no guideline available based on their density, void ratio, plasticity index, standard penetration values, or any other simple soil property; and even more, there is confusion on the influence of clay content, plasticity index, and void ratio. For example, by performing a series tests on loose samples prepared with varying percentages of both plastic and nonplastic fines and nonplastic fine sand, Pitman *et al.* (1994) found that undrained brittleness decreased as the fines content, for both plastic and nonplastic type, increased; at a fines content of 40% the stress path indicated only strain hardening towards steady state. Other research carried out by Ovando-Shelley and Perez (1997) had pointed out that within a limited range of clay content, the presence of clay increases the potential for generating excess pore pressure during undrained loading, and also reduces strength and stiffness.

Therefore, from those researches mentioned above, it could be concluded that the undrained shear behavior of silty soils remains unclear and needs further extensive scrutiny. Therefore, in this research, to study those fluidized landsides where silty soils control the triggering and motion of landslide mass, a series of undrained ring-shear tests was performed on fine-grained sand and the mixtures of this sand with different loess by weight. Based on the tests results, the undrained shear behavior of silty soils was compared, and the undrained peak shear strength and steady state shear

strength were analyzed. Finally, the dissipation of generated pore pressure from the shear zone was examined for liquefied samples with different loess contents.

SAMPLE CHARACTERISTICS

In this research, silica sand no. 8 (S8) was selected as the sample. S8 is a uniform fine-grained sand composed of subangular to angular quartz; its particles have a mean diameter of D_{50} = 0.047 mm, uniformity coefficient of 3.7, maximum void ratio of 1.66, minimum void ratio of 0.85, specific gravity of 2.63. Loess was used also in this research to study the undrained shear behavior of silty soils with different grain size and little plastic fines. This loess, which was composed mainly of silt, was collected from a potential landslide at Lishan, Xi'an, China; its particles have a mean diameter, D_{50} = 0.019 mm, uniformity coefficient of 19.0, maximum void ratio 1.83, minimum void ratio 0.92, specific gravity 2.72, liquid limit 27.0, and plasticity index of 9.5. The grain-size distributions of S8 and loess are shown in Fig. 1. In the present work, a series of tests was conducted on the mixtures of S8 and loess with loess content being 10, 20, and 30 percent, which were termed as M10, M20 and M30, respectively. The corresponding specific gravity was calculated (by weighted average) as 2.63, 2.65, and 2.66, respectively. Their maximum void ratios were measured as 1.51, 1.52, and 1.56, respectively; and minimum void ratios were the same for all mixtures: 0.73.

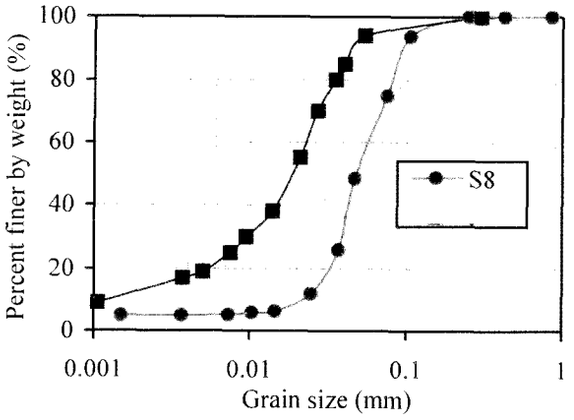

Fig. 1. Grain-size distributions of silica sand no. 8 and loess.

RING-SHEAR APPARATUS AND TEST PROCEDURES

Two new sets of intelligent ring shear apparatus (DPRI-Ver.5 and DPRI-Ver.6) were developed and improved by Sassa and colleagues to simulate the earthquake-triggered-landslides after the Hyogoken-Nammbu earthquake, 17th January 1995, Japan (Sassa 1997). In the present research, DPRI-Ver.6, with a shear box of 250 mm in inner diameter, 350 mm in outer diameter, and 150 mm in height, was employed. The detailed section of half-side undrained ring shear box and the pore pressure measure system is illustrated briefly in Fig. 2.

The oven-dried constituents of the samples were first mixed thoroughly, and then the samples were formed by means of moist placement or dry deposition (Ishihara, 1993), according to different test purposes. The sample was saturated with the aid of carbon dioxide and de-aired water. In all the tests, full saturation was checked using B_D parameter, a saturation degree index in the direct shear state proposed by Sassa (1988). After saturation, all the samples were normally consolidated. And thereafter, undrained shear stress was subsequently applied at a loading rate of 0.098 kPa/sec. Transducers were scanned at a sampling rate of 20 samples/sec. Corresponding to the shear stress control, there are three kinds of rotating gear with final speed of Low (10 mm/sec), Medium (32.3 cm/sec) and High (2.25 m/sec). In this study, the Low gear was selected. To observe the pore pressure generation along shear displacement, all the samples were sheared to a large displacement (usually greater than 10 m).

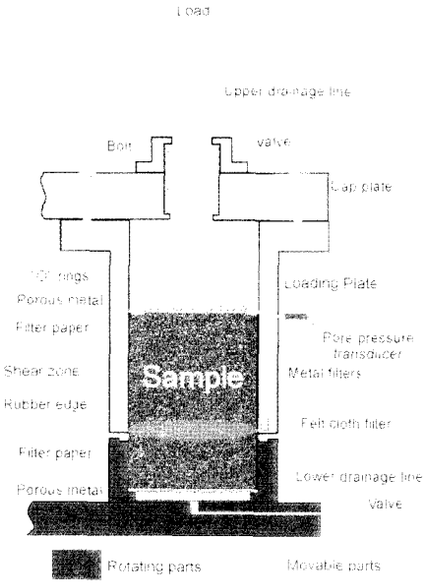

Fig. 2. Undrained shear box and pore pressure measure system for DPRI-Ver.6.

UNDRAINED SHEAR BEHAVIOR

In undrained ring-shear tests, there are two kinds of typical different undrained shearing responses for the samples at different densities. One is the test on loose sand showing effective stress path of mass liquefaction, with quick strain softening process that results in collapse failure; the other is the test on medium/dense sand showing the effective stress path of sliding surface liquefaction, with a process from strain softening to strain rehardening, and finally to strain

softening caused by grain crushing after failure. Here the undrained shear behaviors of different samples will be examined in loose and medium/dense states respectively.

In Loose State

Because of the difficulties in making loose samples, the tests presented here to illustrate the effects of loess content on the undrained shear behavior were different in void ratio and initial normal stress. Nevertheless, the effects could be seen clearly through the tests results. Those selected tests results are plotted in Fig. 3 in the form of effective stress paths (ESP). The results of tests on S8 and M10, which are carried out under initial normal stress of 147 kPa with void ratios being 1.15 and 1.13 respectively, are selected to illustrate the effect of introduction of loess and shown in Fig. 3a. From this figure, it could be seen that the ESP for S8 lies above that for M10, showing that both the peak and steady state shear strengths are greater than those of M10, although the void ratio of S8 is greater than that of M10. It is well known that for a sample under a certain initial stress state, these two strengths are the function of void ratio only; loose sample (greater in void ratio) has smaller peak and steady state shear strengths. Therefore, it could be concluded that these differences are due to the introduction of loess.

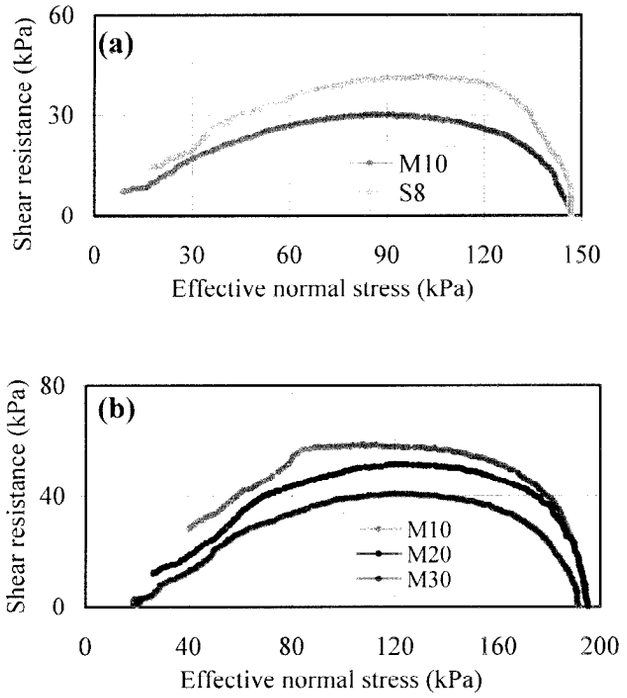

Fig. 3. Comparison of undrained shear behaviors of samples with different loess contents.
(a): Effective stress paths for S8 (e = 1.15) and M10 (e = 1.13); (b): Effective stress paths for M10 (e = 1.10), M20 (e = 1.02), and M30 (e = 1.00).

Three tests on M10, M20, and M30, which are performed under initial normal stress of 196 kPa with void ratio being 1.10, 1.02, and 1.00 respectively, are used to interpret the influence of increasing loess content; and their results are presented in Fig. 3b. As illustrated in this figure, the tests on M30 and M20 showed quick collapse failure after the peak shear strengths were mobilized, while M10 behaved more like a sliding surface liquefaction failure: after the peak shear strength was mobilized, the shear resistance fell downward along the failure line with increasing shear displacement. Meanwhile, it could be found that when the loess content became greater, the corresponding peak shear strength and steady state shear strength became smaller. The test on M30 showed a very small peak shear strength and steady state shear strength (almost tended to 0), showed highest contractiveness potential among these three tests, although the void ratio was the smallest.

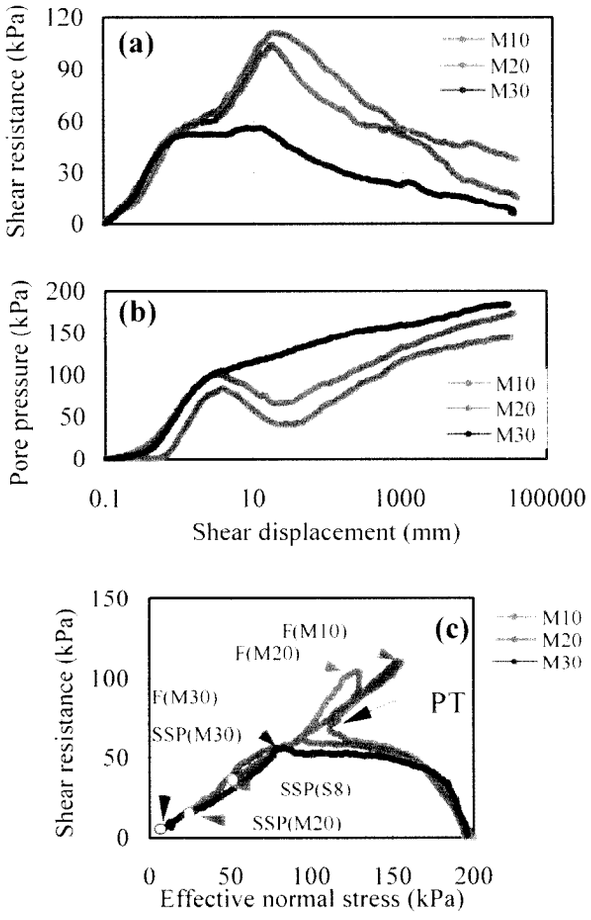

Fig. 4. Results of tests on M10, M20, and M30 in dense state (e = 0.96, 0.89, and 0.89 for M10, M20, and M30, respectively).
(a): Shear resistance against shear displacement;
(b): Pore pressure against shear displacement;
(c): Effective stress paths.

In Dense State

Because no suitable test on dense S8 was obtained for this comparison in dense state, here tests results are just selected to illustrate the influence of increasing loess content (from 10% to 30%) on the undrained shear behavior. Fig. 4 presents the tests results. These tests on M10, M20, and M30 were conducted with initial void ratios of 0.96, 0.89, and 0.89, respectively. To understand the undrained shear behavior of dense sand in ring shear tests, the variation of shear resistance and pore pressure in relation to shear displacement are given in Figs. 4a, b, respectively; Fig. 4c shows the effective stress paths. As shown, with increasing loess content, the undrained shear behavior in the form of effective stress path changed remarkably. The test on dense M10 and M20 showed strong strain rehardening processes after the phase transformation point (point "PT"), during which shear strengths increased greatly due to suction of dense samples, and after failure, shear strengths reduced accompanying the generation of pore pressures (as presented in Figs. 4a, c) due to grain crushing. With increasing loess content, this strain rehardening process becomes weaker, showing a reduction in peak shear strength. For the test on dense M30, there was almost no rehardening process due to dilatancy. This tendency can be seen in Fig. 4b, where the pore pressure generation along with shear displacement showed a continuous increase throughout the whole shearing process without any temporary reduction. Meanwhile, the steady state shear strength becomes smaller with increasing loess content. Therefore, it could be concluded that, with increasing loess content (within the tested range of loess content, 30%), both the peak and steady state shear strength become smaller, while their initial void ratios are the same.

FORMATION OF LOCALIZED FLUIDIZATION IN THE SHEAR ZONE

To observe the shear behavior of these silty sands in ring shear box, the shear deformation was observed after all the tests were finished. After the undrained shear tests, pore water was drained out from the shear box, by flowing air from the upper drainage hose and draining water from the lower drainage valve. By doing this, the sample could be kept relatively undisturbed, while moving the upper mechanical parts of the shear box away. Observation on the shear zone revealed that in all the tests irrespective of the initial densities, an annular shear zone showing allspice-shaped cross section was formed, which was differing from the upper and lower part in color evidently with extinguished interface between its upper and lower boundary, just as that shown in Fig. 2. Meanwhile, grain size analysis revealed that grain crushing just happened within the shear zone. Therefore, it could be inferred that the shearing was centralized along the sliding surface, and then fluidization is limited in the shear zone in ring shear tests, no matter whether the sand was in loose state or in dense state (detailed study on the formation of shear zone and grain crushing could be referred to Wang, 1999).

INTERPRETATION OF THE TESTS RESULTS

Peak Shear Strength

The peak shear strength for a loose sample shows the onset of collapse failure, while that for medium/dense sample shows the start of failure that may be followed by sliding surface liquefaction due to grain crushing. Therefore, the peak shear strength could reflect the potential resistance of a sample to liquefaction. Considering that peak shear strength is dependent on the initial stress state, here those values used to examine the effects of loess content on potential resistance to liquefaction are obtained under the same initial stress state with normal stress being 196 kPa and shear stress being 0. Fig. 5 presents the tests results, where peak shear strengths for S8, M10, M20, and M30 are plotted against void ratios. As reflected in this figure, peak shear strength increases with decreasing void ratio, i.e., when the sample becomes denser, as expected. Meanwhile, from this trend of each sample one could see that given the void ratio being the same, the peak shear strength becomes smaller with increasing loess content, also as expected. Therefore, it is concluded that with increasing loess content, the liquefaction resistance decreases, i.e., the sample becomes easier to suffer liquefaction failure (within the tested range of loess content: 30%).

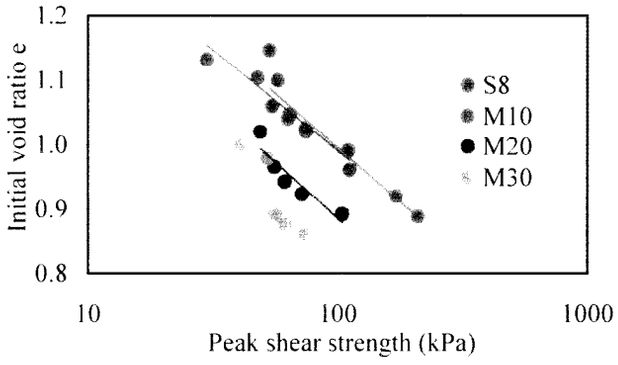

Fig. 5. Peak shear strength against void ratio.

Steady State Strength

The steady state strengths for S8, M10, M20, and M30 are presented in Fig. 6, where void ratios are plotted as ordinates, and shear strengths and effective normal stresses at steady state as abscissas in logarithm form. As seen, with increasing loess content, the steady state line shifts the position from that of the host sample of S8; when the void

ratios for each of these samples are the same, the shear strength at steady state becomes smaller with increasing loess content, at least within the range of loess content of 30%.

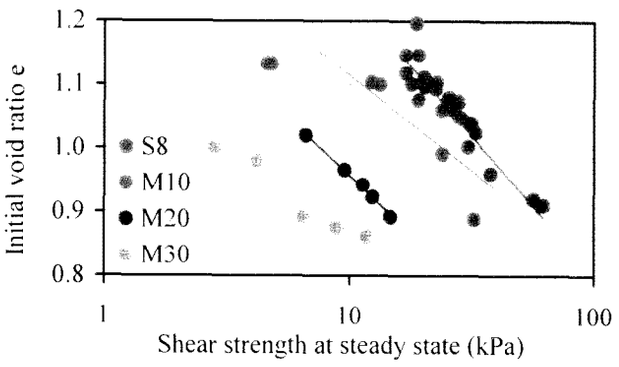

Fig. 6. Shear strength at steady state against void ratio.

From these test results on the mixtures of S8 with different loess contents by weight, it could be concluded that adding loess to the sand in certain extent could increase the liquefaction potential of sand due to the contributions in at least two aspects: (1) reducing the liquefaction resistance that would make sand more easily to liquefy; and (2) reducing the steady state shear strength that could be connected with smaller apparent friction angle (a concept that could be connected with the final motion state of liquefied soils and defined as the ratio of steady state shear strength against initial normal stress in ring-shear test (Sassa, 1985)) with larger run-out distance for a fluidized landslide in the practical situation.

MAINTAINING GENERATED PORE PRESSURE IN SHEAR ZONE

In practice, there were many cases where liquefaction has been initiated but liquefaction-induced movements were of only limited extent (Seed, 1968). Although there are many reasons why a slide caused by soil liquefaction may not result in large deformations, maintenance of generated pore pressure may be the most important factor. Liquefaction can only persist as long as high pore pressures persist in a soil; if drainage can occur rapidly then liquefaction may persist for such a short period of time that large displacements are unable to develop. In practice, the liquefied soil mass could be regarded as in undrained conditions during the very short period of failure triggered by earthquake, rainfall or some other factors, but could not be treated as in undrained condition throughout the whole translation process. Therefore, the persisting of generated pore pressure will be an important factor affecting the run-out distance of a fluidized landslide in the field, just as stated by Seed (1968). Considering that in this ring shear test series and in many historic liquefaction failures, liquefaction was limited in the shear/slide zone, it is highly desirable to have an insight into the maintenance of pore pressure in the shear zone. Therefore, a series of ring shear tests was carried out to examine the effects of loess content on the dissipation of generated pore pressure from the shear zone. During tests, the saturated samples were sheared in undrained conditions to a large displacement where the liquefaction was ensured to have been initiated. Thereafter the shear box was permitted to drain to observe the dissipation of generated pore pressure and recovery of shear strength.

Figure 7 presents the results of tests on S8, M10, M20, and M30, where the shear resistances are plotted against the elapsed time. In all these tests, the moment when the shear box was turned into drained condition was treated as the zero point of elapsed time. Because the pore pressure transducers recorded pore pressure outside the shear zone (as illustrated in Fig. 2), when the shear box was turned into a drained condition, the pore pressure within the shear zone could not be observed correctly. Nevertheless, the recovery of shear strengths could reflect the dissipation of generated pore pressure. As shown in Fig. 7, when the shear box was turned into a drained condition, the shear strengths of S8, M10, M20 recovered with elapsed time, i.e., with the dissipation of generated pore pressure. However, an observation on the inclination of each curve (recovering rate of shear strength) led to the finding that as the loess content became greater, the recovery rate of shear strength was smaller. This is especially the case for the test on M30, where there was almost no recovery tendency that could be seen. Therefore, it could be inferred that once the liquefaction was initiated in the soil mass containing greater fines with smaller grain size (similar to those in M30), the pore pressure could be maintained for a long time and that this would result in large deformation. This result showed consistency with many laboratory research results and field cases (Seed, 1968; Zeng and Arulanandan, 1995).

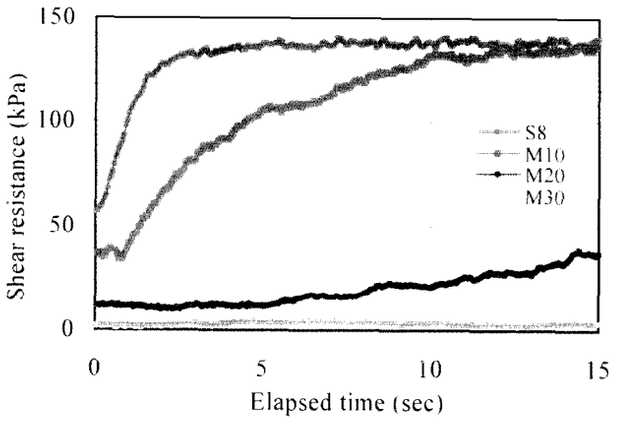

Fig. 7. Recovery of shear strength for liquefied samples after the shear box was turned into drained condition.

CONCLUSIONS

A series of tests was conducted on a uniform, fine-grained sand and the mixtures of this sand with different loess contents to study the undrained shear behavior of silty sands in ring-shear tests. By performing the tests at different initial void ratios, the undrained shear behavior of samples with different loess contents at loose and medium/dense states were presented and discussed. Based on the test results, effects of loess content on the peak and residual shear strengths were examined. Finally, effects of loess content on the dissipation of pore pressure generated in the shear zone were examined also.

The findings obtained from these tests results could be summarized as follows.

1. Adding loess to fine-grained sand could change the grain size and content of plastic fines, and then change the undrained shear behavior greatly.

2. With increasing loess content in the mixture, both the peak shear strength and steady state shear strength decrease while their initial densities being the same. In the test with the addition of 30% loess in a loose state, the steady state shear strength dropped to approximately 0; meanwhile, tests on the same mixture in a denser state show that there is almost no re-hardening process in shear strength in M30, even though in dense state.

3. With increasing loess content, the dissipation of generated pore pressure within the shear zone becomes slower when the shear box was permitted to drain. Results of testing on fine-grained sand with 30 percent loess showed that the generated high excess pore pressure remained within the shear zone for a long time with little if any dissipation, even though the shear box was in drained condition.

Finally, it is worth noting that the undrained shear behavior of silty soils is not very clear at present, and the tests results presented here are quite limited. Further studies on the synthetic effects of grain size and plastic fines on the undrained shear behavior of silty soils are needed and scheduled in the future.

REFERENCES

Bishop, A.W. [1973]. "The stability of tips and spoil heaps". *Q. J. Engrg. Geol.* 6, 335-376.

Eckersley, J. D. [1990]. "Instrumented Laboratory Flowslides". *Géotechnique* 40, No. 3, 489-502.

Guo, T. and Prakash, S. [1999]. "Liquefaction of silts and silt-clay mixtures". *Journal of Geotechnical and Geoenvironmental Engineering*, ASCE, Vol. 125, No. 8, pp. 706-710.

Ishihara, K., Okusa, S., Oyagi, N., and Ischuk, A. [1990]. "Liquefaction-induced flowslide in the collapsible loess deposit in Soviet Tajik". *Soils and Foundations* Vol. 30, No. 4, 73-89.

Ishihara, K. [1993]. "Liquefaction and flow failure during earthquakes". *Géotechnique* 43(3), 349-451.

Ovando-shelley, E., and B. E. Perez. [1997]. "Undrained behaviour of clayey sands in load controlled triaxial tests". *Géotechnique* 47, No. 1, 97-111.

Pitman, T. D., Robertson, P. K., and Sego, D. C. [1994]. "Influence of fines on the collapse of loose sands". *Can. Geotech. J.* Vol. 31, pp. 728-739.

Sassa, K. [1985]. The mechanism of debris flows. *Proc., XI Int'l. Conf. Soil Mech. Found. Engrg.*, San Francisco, 3, 1173-1176.

Sassa, K. [1988]. "Geotechnical model for the motion of landslides". Special Lecture of 5th International Symposium on Landslides, "*Landslides*", **1**. Rotterdam: Balkema. 37-55

Sassa, K. [1996]. "Prediction of earthquake induced landslides". Special Lecture of 7th International Symposium on Landslides, "*Landslides*", Rotterdam: Balkema, **1**, 115-132.

Sassa, K. [1997]. "A new intelligent type of dynamic loading ring-shear apparatus". *Landslide News*. No.10, pp.33.

Seed, H. B. [1968]. "Landslides during earthquakes due to soil liquefaction". *Journal Soil Mechanics Foundations Division, ASCE*, 94, No. 5, 1055-1122.

Zeng, X. and Arulanandan, K. "Modeling the Lateral Sliding of a Slope due to Liquefaction of a Sand layer," *Journal of Geotechnical Engineering*, ASCE, Vol. 121, No.11, 814-817, 1995.

Zlatovic, S. and Ishihara, K. [1995]. "On the influence of nonplastic fines on residual strength". *Proc., IS-TOKYO'95, 1st Int. Conf. on Earthquake Geotech. Engrg.*, K. Ishihara, ed., A. A. Balkema, Rotterdam, The Netherlands, 239-244.

Wang, G. H. [1999]. "*An experimental study on the mechanism of fluidized landslide – with particular reference to the effect of grain size and fine-particle content on the fluidization behavior of sands*". PhD Thesis. Kyoto University.